ELECTRONIC STRUCTURE AND PROPERTIES

The Symmetry of Rare-Earth Metals. The Paradox of Ce and Its Alloys. Quantum Theory. I. Ce

O. I. Mitsek and V. M. Pushkar

*G. V. Kurdyumov Institute for Metal Physics, N.A.S. of Ukraine,
36 Academician Vernadsky Blvd.,
UA-03680 Kyiv, Ukraine*

The symmetry of rare-earth metals (REM) and f.c.c.-Ce 'paradox' are calculated by means of the method of many-electron operator spinors (MEOS). Spin and orbital MEOS factors with [0001] axis of quantization of the angular moment $\mathbf{J}$ are responsible for hexagonal deformation $\Delta(c/a) \propto J^2$. Indirect covalent $4f$–$4f$ bond via band fermions adds the bond energy $E_{4f} \propto n_f$. Covalent electron collectivization ($n_f = 2$) for Ce($4f^2$) gives $\mathbf{J} \to \mathbf{0}$ and $\Delta(c/a) = 0$. In the REM-Ce, there is instability of $4f$-shell contributing to the appearance of $5d$-states with amplitude $\xi_d(T)$. Covalent bond $\Gamma^{dd}(\mathbf{k})$ (in the MEOS method) appears because of the chemical-bond fluctuations (CBF) for temperature $T > T_+$ in the form of $\xi_d(T > T_+)$ jump. Hysteresis of the f.c.c.–f.c.c. α–γ-transition is caused by the band–covalent bond $\gamma_{b\text{-}c}$. Its maximum width $\Delta T_h \propto \gamma_{b\text{-}c}^{2/3}$ determines jumps of the volume $\Delta\omega(T_+)$, entropy $\Delta S(T_+)$, electrical resistance (ER) $\Delta R(T_+)$, etc. Particularly, the ER jump $\Delta R(T_+) \propto \Delta T_h$. The experimental data are interpreted by the use of results of calculation.

Методом багатоелектронних операторних спінорів (БЕОС) розраховується симетрія рідкісноземельних металів (РЗМ) разом із «парадоксом» ГЦК-Се. Спінові й орбітальні фактори БЕОС з віссю [0001] квантування кутового моменту $\mathbf{J}$ відповідальні за гексагональну деформацію $\Delta(c/a) \propto J^2$. Непрямий ковалентний $4f$–$4f$-зв'язок через зонні ферміони додає енергію зв'язку $E_{4f} \propto n_f$. Ковалентна колективізація $n_f = 2$ для Ce($4f^2$) занулює $\mathbf{J} \to \mathbf{0}$ і дає $\Delta(c/a) = 0$. В РЗМ-Се виникає нестабільність $4f$-оболонки, що сприяє появі $5d$-станів з амплітудою $\xi_d(T)$. Ковалентний зв'язок $\Gamma^{dd}(\mathbf{k})$ (в методі БЕОС) з'являється як результат флюктуацій хемічних зв'язків (ФХЗ) за температури $T > T_+$ у формі стрибка $\xi_d(T > T_+)$. Гістерезу α–γ-переходу ГЦК–ГЦК зумовлено зонно-ковалентним зв'язком $\gamma_{b\text{-}c}$. Її максимальна ширина $\Delta T_h \propto \gamma_{b\text{-}c}^{2/3}$ визначає стрибки об'єму $\Delta\omega(T_+)$, ентропії $\Delta S(T_+)$, електроопору (ЕО) $\Delta R(T_+)$ тощо. Зокрема, стрибок ЕО $\Delta R(T_+) \propto \Delta T_h$. Результатами розрахунків проінтерпретовано експериментальні дані.

Методом многоэлектронных операторных спиноров (МЭОС) рассчитыва-

ется симметрия редкоземельных металлов (РЗМ), включая «парадокс» ГЦК-Ce. Спиновые и орбитальные факторы МЭОС с осью [0001] квантования углового момента $\mathbf{J}$ ответственны за гексагональную деформацию $\Delta(c/a) \propto J^2$. Косвенная ковалентная $4f$–$4f$-связь через зонные фермионы добавляет энергию связи $E_{4f} \propto n_f$. Ковалентная коллективизация $n_f = 2$ для Ce($4f^2$) обнуляет $\mathbf{J} \to \mathbf{0}$ и даёт $\Delta(c/a) = 0$. Возникающая в РЗМ-Ce нестабильность $4f$-оболочки способствует появлению $5d$-состояний с амплитудой $\xi_d(T)$. Ковалентная связь $\Gamma^{dd}(\mathbf{k})$ (в методе МЭОС) появляется как результат флюктуаций химических связей (ФХС) при температуре $T > T_+$ в форме скачка $\xi_d(T > T_+)$. Гистерезис α–γ-перехода ГЦК–ГЦК обусловлен зонно-ковалентной связью $\gamma_{b\text{-}c}$. Его максимальная ширина $\Delta T_h \propto \gamma_{b\text{-}c}^{2/3}$ определяет скачки объёма $\Delta\omega(T_+)$, энтропии $\Delta S(T_+)$, электросопротивления (ЭС) $\Delta R(T_+)$ и т.п. В частности, скачок ЭС $\Delta R(T_+) \propto \Delta T_h$. Результатами расчётов проинтерпретированы экспериментальные данные.

1. INTRODUCTION

Structures of the rare-earth metals are determined by the symmetry of the covalent bonds, H^{cov}. Isotropic coordinate parts of these $3d$–$3d$-bonds stabilize cubic phases of the Fe-group. 'Sea' of band electrons contributes to enhancement of the symmetry up to f.c.c. or b.c.c. phase, particularly, by H^{cov} screening. Falling in magnetic symmetry by the induction of magnetic order of $\mathbf{S}_r$ spin system of the lattice sites, $\mathbf{r}$ weakly reduces the total symmetry due to the isotropy of exchange bonds $(\mathbf{S}_r$–$\mathbf{S}_R)$ [1–3]. Delocalization collectivization of the covalent electrons [4] and their spins $\mathbf{S}_r$ confirms high symmetry. The last is weakly distorted by the localization of $\mathbf{S}_r$ (Co, Mn, *etc.*).

An alternative picture is for REM Pr–Tm. The locality of magnetism carriers $\mathbf{S}_r$ and $\mathbf{L}_r$ [1, 2] of $4f$-sublattice, as we will see below, leads to the strong compression along the [0001], $\varepsilon_{33} \cong 0.1$. The universality of h.c.p. compression requires universal explanation as its exception (Ce and Yb). Here, two contrary technical aspects arise: (i) strong magnetic anisotropy of REM compounds as permanent magnets and undying interest to its details (see, *e.g.*, [5] as well as [6, 7]); and (ii) shape memory of Ce alloys (works of the group of Yu. M. Koval [8] *et al.*). The isomorphic transition in cubic Ce [1] and its alloys at the temperatures $T \cong 300$ K is convenient for application.

Their strong spin−orbit coupling (*s-o*) approves unitary action $\mathbf{S}_r$ and $\mathbf{L}_r$ on symmetry of REM. The nature of *s-o* (particularly, its sign reversal for transition from heavy to light RE ions (REI)) requires

elaboration of theory beyond the simple Bohr model of atomic shells. Here, we try to give a more precise definition (introduce clarity) to the theory within the framework of MEOS method [4, 6, 7]. We will rely on the hypothesis of indirect (exchange and others) bonds. Here, we consider as those $4f-6s$-bonds through bond $(6s)$ electrons. This bond establishes a magnetic order, which is rather difficult [1] except of ferromagnetic-only (FM) Gd ($L = 0$), but always relates to [0001].

The paradox of Ce consists in the absence of magnetic order, in spite of the presence of ($4f^2 6s^2$) (spin $S = 1$) 'conditional' $4f$-shell. There is no an h.c.p. distortion, although there is a deformation for Ce−Al and other alloys [8].

The paper is arranged as follows. In Section 2, we discuss the nature of h.c.p. deformation. The Ce paradox is solved in Sec. 3 by the introduction of $f-s$ hybridization of REI in a metal. Also in Sec. 3, we calculate first-order isomorphic f.c.c.−f.c.c. transition and reveal role of the band−covalent bonds for width of its hysteresis area. Electrical resistance (ER) jump for isomorphic transition is calculated in Sec. 4. Generalization to Ce alloys is discussed in Sec. 5. Finally, summary and conclusions are given in Sec. 6.

2. THE SYMMETRY OF REM

The REM lattice consists of RE ions ($4f^{n_f} 5d^{n_d} 6s^2$). We represent the REI by the many-electron operator spinors (MEOS) [4, 6, 7] in a form of the wave function

$$\psi_r^+ = \xi_f F_r + \xi_d D_r + \sum_\sigma \xi_\sigma f_{r\sigma}^+ , \qquad (2.1)$$

which consists of the f, d, and s components—electrons with spins σ.

The MEOS for $4f$ shell:

$$F_r = \{F_{r\sigma L} c_{r\sigma} v_{rL}\}, \quad F_{r\sigma L} = \prod_{\mu=1}^{n} a_{\mu\, r\sigma L}, \quad c_{r\sigma}^2 = \frac{1 + \sigma S_r}{2}, \quad v_{rL}^2 = \frac{1 + LL_r}{7}, \qquad (2.2)$$

where $n = n_f \le 7$. Orbital moment $|\mathbf{L}| \le 3$ and $|\mathbf{S}| \le 7/2$.

The MEOS for virtual $5d$-electrons, which are real for Gd ($n_d \le 1$):

$$D_r = \{d_{r\sigma}\}, \quad L_r = 0, \quad (D_r^+ = \bar{D}_r), \quad D_r \bar{D}_r = F_r \bar{F}_r = 1 . \qquad (2.3)$$

These conditions of locality of covalent electrons allow to introduce unambiguously and rigorously fluctuations of the chemical (here, covalent) bonds (FCB) via the Fourier series (for given σ and $\mathbf{L}$)

$$F_r = F_0 + \sum_k F_k e^{ikr}, \quad F_k = \sum_r F_r e^{-ikr} \Big/ N , \quad f_k = \sum_r f_r e^{ikr} , \qquad (2.4)$$

where N is a density of the lattice sites.

Covalent bond is indirect via the band electrons f_r.

$$H^{\text{cov}-e} = -\sum \Gamma^{fe}(r - R)F_r f_R^+ f_r \overline{F}_R, \quad \Gamma^{fe}(k) = \sum_r \Gamma^{fe}(r)e^{ikr}. \qquad (2.5)$$

Substituting Eq. (2.2) and expanding spin and orbital factors over the operators of spins $\mathbf{S}_r$ and moments $\mathbf{L}_r$, we start from zero term and obtain

$$H^{\text{cov}-e} = H_0 + \Delta H(u_{jj}), \quad \Gamma^{fe}(u_{jj}) = \Gamma^{fe}(0) + \Gamma_{jj}^{fe}u_{jj}, \quad \Gamma_{jj}^{fe} = \partial\Gamma^{fe}/\partial u_{jj}. \quad (2.6)$$

The second term in Eq. (2.6) appears only taking into account vector components of MEOS,

$$\Gamma_{jj}^{fe}(r) = (\partial\Gamma^{fe}/\partial r_j)(\sigma_j^2 S_{rj}^2 q + L_i^2 L_{rj}^2 q_L), \quad r_j = r_{0j} + a_j u_{ij}, \qquad (2.7)$$

where a_j is a lattice parameter.

One can obtain deformation u_{ij} via introducing the quantization axe (here, $0z \parallel [0001]$). Let us use a postulate (Hund rule) on dominance of the Hund energy (*e.g.*, over the Hubbard repulsion) and localization $\mathbf{S}_r = \mathbf{S}$. One more attribute of REM (strong spin−orbit coupling *s-o*) create a local moment $\mathbf{L}_r \parallel \mathbf{S}_r$ (for heavy REI, where $H^{s\text{-}o} < 0$) or $\mathbf{L}_r \uparrow\downarrow \mathbf{S}_r$ for light REI ($H^{s\text{-}o} > 0$). This allows introducing a total angular moment $\mathbf{J} = \mathbf{S} + \mathbf{L}$. Variation of thermodynamic potential $\Phi(\hat{\mathbf{u}})$ with an account of elastic moduli C gives unitary value for REM

$$u_{jj} = u_{zz}\delta_{jz} = \left\langle \Gamma_{zz}^{fe} \right\rangle (J_r^z)^2 \big/ C. \qquad (2.8)$$

Note that Ce is paradoxically omitted from this general result (h.c.p. structure of REM), which also includes b.c.c. Eu ($\mathbf{S} = -\mathbf{L}$, $\mathbf{J} = 0$); see Table.

For a qualitative comparison of theory with experiment, in the Table, we give data for an angular moment of REI^{3+} [9] in a form of J_z^2 and h.c.p. deformation in a form of the relation modulo $(c/a) - 1.633$ (compression of u_{zz} along [0001]). Correlation of the tabular data and theoretical fit (2.8) is obvious. (Here, we do not give data for the moments of Ce^{3+} and Yb^{3+}, which strongly disagree with those for corresponding pure REM.) It is obviously also that different normalization of c_σ^2 and v_L^2 is not taking into account explicitly during universalization of Eq. (2.8). Therefore, difference in the contribution of the moments $\mathbf{S}$ and $\mathbf{L}$ into the total expression (2.8) should be included carefully taking into consideration band structure and band−covalent bonds (2.5).

Paradoxical missing of Ce out of general series of REM is caused by the sharp distinction of REI in a metal and REI^{3+} (data for which are

not listed in the Table). It is quite clear cubic structure of such REM as Eu ($4f^7 6s^2$, at $\mathbf{S} = \mathbf{0} = \mathbf{L}$) and Yb ($4f^{14} 6s^2$). Theory resolves the paradox of f.c.c. Ce proving vanishing of $\mathbf{S} = \mathbf{0} = \mathbf{L}$ during the crystallization (see below).

3. F.C.C. LATTICE OF Ce^{58}($4f^2 6s^2$) ISOMORPHISM

Let us start considering of the paradox of f.c.c. Ce from the analysis of REI. Its internal structure requires going beyond the scope of the atomic Bohr model and explicit introduction of f−s and f−d hybridization. In the MEOS representation (2.1), for $n_d = 2$, the local Hamiltonian of REI

$$H_r = -E_{4f} F_r \bar{F}_r \xi_f^2 - E_{5d} \xi_d^2 D_r \bar{D}_r - \xi_d \xi_f (g F_r \bar{D}_r + H.c.) +$$
$$+ (U_d \xi_d^4 / 2) + U_s F_r f_{r\sigma}^+ f_{r\sigma} \bar{F}_r . \tag{3.1}$$

Here, the last two terms of the Hubbard repulsion ($U_d > 0$ and $U_s > 0$) restrict localization of the 5d- and 6s-shell. Spin component of the last term favours the antiparallel spin orientation $\mathbf{S}_r \uparrow\downarrow \mathbf{s}_r$ of 4f- ($\mathbf{S}_r$) and 6s-($\mathbf{s}_r$) shells. Due to the equality of their filling (two electrons at each shell), the total spin of REI in REM lattice vanishes ($\mathbf{S} = \mathbf{0}$). Strong spin−orbit coupling ($\alpha > 0$) annihilates the resulting orbital moment of REI in REM, in contrast to REI^{3+} [9], in agreement with experiment and Eq. (2.8).

We research the genesis of Ce isomorphism using numerous assumptions [9] of 'unfreezing' of 5d-electrons. Previous studies had no basis for mathematical treatment of this idea. In our MEOS-based CBF-method, the calculation of effects associated with isomorphism of REM-Ce is consistent and strict enough. We proceed from the covalent 5d−5d and band−covalent d−s bonds:

$$H^{cjv} = -\sum_{rR} \xi_d^2 \Gamma(r - R) D_r \bar{D}_R - \xi_d \sum_{rRt} (\gamma D_r f_R f_t + H.c.) , \tag{3.2}$$

where Fourier series

$$D_r = D_0 + \sum_k D_k e^{ikr}, \ \ D_k = \sum_r D_r e^{-ikr} / N \xi_d^2, \ \ [D_k, \bar{D}_q]_- = \delta_{kq} / N \xi_d^2. \tag{3.3}$$

TABLE. Values for $|u_{zz}| = (1.633 - c/a) \cdot 10^3$.

REI	Ce	Pr	Nd	Sm	Eu	Gd	Tb	Dy	Ho	Er	Tm	Yb
$\mathbf{J}^2$	–	12	12	11	0	64	100	102	102	90	53	–
$|u_{zz}|$	0	22	20	26	0	39	53	57	58	60	58	0

Bose operators D_k give CBF for $5d$-electrons.

In the interior of Ce-ion, we have to add to Eq. (3.2) energy of the $5d$-shell in a representation (3.3)

$$\Delta H_r = -E_{5d}(1 - D_0\bar{D}_0)\xi_d^2 \text{ and } E_{dk} = E_{5d} + \Gamma(k) \cong \Gamma_0 + \Gamma k^2. \qquad (3.4)$$

Density of CBF (N_k) is determined by the screening $\Gamma(k)$ with radius scales as $1/k$

$$N_k = \left\langle D_k\bar{D}_k \right\rangle, \ \Gamma(k) = \Gamma/(k^2 + \kappa^2) \cong \Gamma(0) - \Gamma_k. \qquad (3.5)$$

Bose statistics of CBF (3.5),

$$N_k = [\exp(\beta E_{dk}) - 1]^{-1} \cong 1/(\beta E_{dk}), \ \beta = 1/(k_B T), \qquad (3.6)$$

results in covalent part of thermodynamic potential (TDP)

$$\Phi^{\text{cov}} = \left\langle H^{\text{cov}} \right\rangle = -\xi_d^2 \sum_k \Gamma(k)N_k \cong -\xi_d^2 I_d/\beta, \qquad (3.7)$$

where integral

$$I_d = \sum_k \Gamma(k)/E_{dk} \propto \Gamma/E_{5d} \cong 0.1 \text{ eV}/1 \text{ eV} \cong 0.1,$$
$$E_{4f} - E_{5d} = E_{fd}. \qquad (3.8)$$

Estimation of small value I_d (3.8) allows now quantization of CBF with band spectrum.

Transform Eq. (3.2) into **k**-representation

$$H^{c-b} = \xi_d \sum_k \{\gamma_{k0}D_0 f_k f_{-k} + \sum_q \gamma_{kq}D_q f_k f_{q-k} + H.c.\} + \sum_k \tilde{\varepsilon}_k f_k^+ f_k \qquad (3.9)$$

and introduce Green functions (of Bogolyubov type) taking into account their further using during calculation of ER jump,

$$G_k^f = \left\langle\left\langle f_k(f_{-k}^+) \mid f_k^+ \right\rangle\right\rangle, \ G_{rq(0)}^{df} = \left\langle\left\langle \bar{D}_{q(0)}f_{q-k}^+ \mid f_k^+ \right\rangle\right\rangle. \qquad (3.10)$$

Motion equation (3.10)

$$\begin{pmatrix} (E - \tilde{\varepsilon}_k) & \gamma_k^*\xi_d \\ \gamma_k/\xi_d & (E - \Gamma_0) \end{pmatrix} \begin{pmatrix} G_k^f \\ G_{k0}^{df} \end{pmatrix} = \begin{pmatrix} 1 - \sum_q \gamma_{kq}G_{kq}^{df} \\ 0 \end{pmatrix}, \qquad (3.11)$$

and also

$$(E - \Gamma_q)G_{kq}^{df} + \xi_d\gamma_{kq}(N_q - n_{k-q}/\xi_d)G_k^f = 0, \ n_k = \left\langle f_k^+ f_k \right\rangle, \qquad (3.12)$$

where a density of band electrons, n_k, is introduced.

Note renormalization of the band spectrum,

$$\varepsilon_k^{(1)} = \tilde{\varepsilon}_k \pm (|\gamma_k|^2/\tilde{\varepsilon}_k) - \sum_q [\gamma_{kq}^2/(E - \Gamma_q)](n_{k-q} - \xi_d N_q), \qquad (3.13)$$

and correlator

$$K_{df}(q) = \left\langle f_{k-q}^+ f_k^+ \bar{D}_q \right\rangle = \gamma_{kq}(n_{k-q} - \xi_d N_q)N_q, \ \ K_{df}(0) = \gamma_k n_k/\tilde{\varepsilon}_k. \quad (3.14)$$

Its contribution

$$\Delta\Phi = -\gamma\xi_d, \ \ \gamma = \sum_k (|\gamma_{k0}|^2/\tilde{\varepsilon}_k)n_k \propto |\gamma|^2/\varepsilon_F \qquad (3.15)$$

into the TDP contains combination of γ-factors (3.15) after averaging of (3.9).

Taking into account Eq. (3.5) and Eqs. (3.9)–(3.15), one can write the TDP as

$$\Phi = (U_d/2)\xi_d^4 + (T_{c+} - T)\xi_d^2 A - \gamma\xi_d, \qquad (3.16)$$

where the fixed point of the first-order transition

$$T_{c+} = E_{fd}/k_B, \ \ A = I_d k_B. \qquad (3.17)$$

Variation of $\Phi(\xi)$ yields $(\xi_d = \xi)$

$$U\xi^2 - \tau_+ - \gamma/\xi = 0, \qquad (3.18)$$

or

$$\Phi_{\xi\xi}'' = 6U\xi^2 - 2A\tau_+ > 0, \qquad (3.19)$$

i.e. for $\tau_+ = T - T_{c+} < 0$, $\xi = 0$. Solution of Eq. (3.19) corresponds to low-temperature f.c.c. phase of Ce.

Hysteresis of the transition can be calculated introducing its width τ_h,

$$\Delta T_h = \tau_h = T_{c+} - T_{c-} = \tau, \qquad (3.20)$$

from the equation

$$A\tau + \tilde{\gamma}(U/A)^{1/2}/\tau^{1/2} = 0, \ \ \tilde{\gamma} \propto \gamma. \qquad (3.21)$$

Hence width of loop ΔT_h (3.20) of hysteresis of α–γ-transition in Ce has a form:

$$\tau = (\tilde{\gamma}^2 U)^{1/3}/A \,. \tag{3.22}$$

Substituting (3.22) into (3.18), we obtain amplitude jump of $5d$-states

$$\xi_d^2(h) = \xi_+^2(T_{c+}) = 2(\tilde{\gamma}/U)^{2/3} \,, \tag{3.23}$$

that allows calculation of jump $\Delta\omega(T)$ for transition.

The last can be found via introducing of mechanical part of TDP ($\Gamma' \propto \partial\Gamma/\partial\omega$, C—elastic module),

$$\Delta\Phi(\omega) = (C/2)\omega^2 - \Gamma'\omega\xi_+^2 \,, \tag{3.24}$$

that gives

$$\omega_+(T_{c+}) = 2(\Gamma'/C)(\gamma/2U)^{2/3} \,. \tag{3.25}$$

Subsequent growth of the volume for $T > T_{c+}$,

$$\Delta\omega(T) = \Gamma'\xi^2(T) = (\Gamma'A/CU)(\tau_+ + q/\tau_+^{1/2}) \,, \tag{3.26}$$
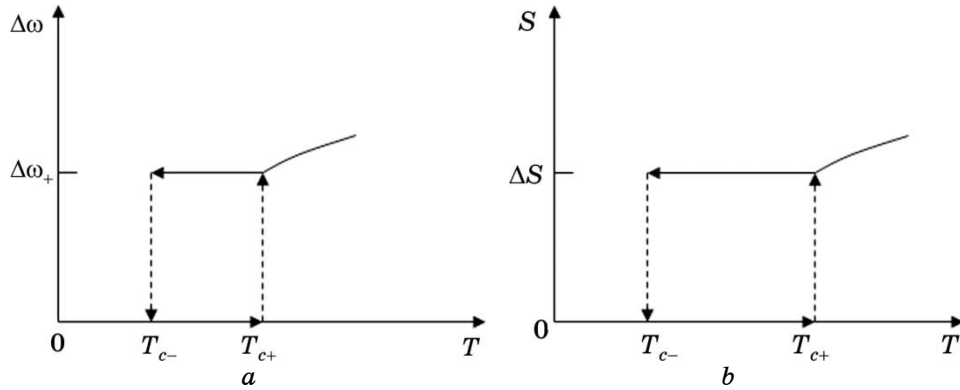
scales nonlinearly with T (Fig. 1, a).

We find entropy S from the total TDP

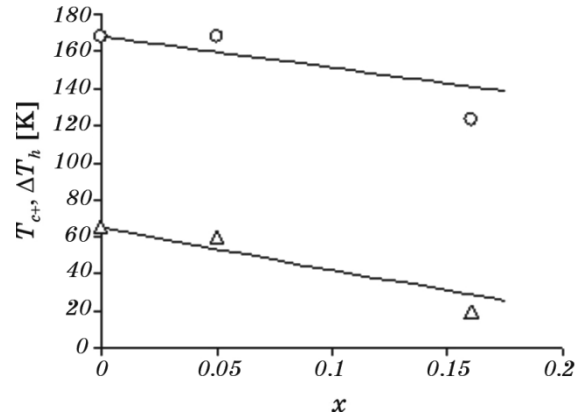$$\Phi \cong (A^2/2U)(T - T_{c-})^2, \quad S = -\partial\Phi/\partial T = -(A^2/U)(T - T_{c-}), \tag{3.27}$$

and its jump for α–γ transition (Fig. 1, b),

$$\Delta S(T_{c+}) = -[(I_d k_B)^2/U]\Delta T_h \,. \tag{3.28}$$

Fig. 1. Enhancement of the volume $\Delta\omega$ (*a*) and change in the entropy $S(T)$ (*b*) *vs.* temperature T for α–γ-transition in Ce.

Fig. 2. Dependences of temperature of $\alpha-\gamma$-transition $T_{c+}(x)$ ($\circ$) and width of its hysteresis $\Delta T_h(x)$ ($\triangle$) for $Ce_{1-x}Al_x$. Experimental data are adapted from Ref. [8].

Calculated jumps of the volume (3.25), entropy (3.28), and further ER are expressed by the width of hysteresis ΔT_h (3.22). Comparison with experimental data from Ref. [8] is shown in Fig. 2.

4. ELECTRICAL RESISTANCE AND ITS JUMP, $R(T_{c+})$

Experiment helps us to connect data for jumps of the volume $\Delta\omega(T_{c+})$ (Fig. 1, *a*), entropy $\Delta S(T_{c+})$ (Fig. 1, *b*) and electrical resistance during $\alpha-\gamma$-transition. Appearance of the covalently bonding $5d$-electrons (D_r) and their CBF (D_k) adds after-transition mechanism of scattering of bond electrons. Additional Hamiltonians of the scattering ($\xi_d = \xi$)

$$\Delta H^{c-b} = \xi\left\{\sum_{kq}[\gamma_1(k,q)D_q f_k f_{q-k} + \xi\gamma_2(k,q)D_q f_k^+ \bar{D}_0 f_{k+q}] + H.c.\right\} \quad (4.1)$$

introduce two mechanisms of $s-d$-scattering. In addition to Green functions (3.10), we add

$$G_{kq}^{df2} = \left\langle\left\langle D_0\bar{D}_q f_{k+q} \mid f_k^+\right\rangle\right\rangle \quad (4.2)$$

for the second scattering mechanism.
   Two systems of motion equations are

$$\begin{cases} (E - \tilde{\varepsilon}_k)G_k^f + \xi\gamma_{1k}G_{k0}^{df} + \xi\sum_q[\gamma_1(k,q)G_{kq}^{df} + \xi\gamma_2 G_{kq}^{df2}]N = 1, \\ (E + \tilde{\varepsilon}_k)G_{k0}^{df} + \xi\gamma_{1k}\rho_0^2 G_k^f + \ldots = 0. \end{cases} \quad (4.3)$$

and also (E_q—CBF energy)

$$\begin{cases} (E - \tilde{\varepsilon}_{q-k} - E_q)G_{kq}^{df} - n_{q-k}G_k^f\gamma_1(K, q)/\xi + \dots = 0, \\ (E - \tilde{\varepsilon}_{r-q} - E_q)G_{kq}^{df2} - \rho_0^2 n_{k-q}\gamma_2(K, q)G_k^f/\xi = 0, \quad \rho_0^2 = \left\langle D_0\bar{D}_0\right\rangle. \end{cases} \tag{4.4}$$

Using Eqs (4.4) and (4.3), we obtain renormalization (3.13) of band spectrum with addition from the second mechanism

$$\Delta\varepsilon_{k2} = -\rho_0^2\sum_q \frac{N_{k-q}\gamma_2(k, q)}{E + E_q - \tilde{\varepsilon}_{k-q}}. \tag{4.5}$$

Its imaginary part (IP) gives scattering on the CBF (E_{k-q})

$$\operatorname{Im}\tilde{\varepsilon}_k \cong 2\pi\rho_0^2\xi^2\sum_q \gamma_2(k, q)n_B(E_{k-q})\delta(\varepsilon_k + E_q - \varepsilon_{k-q}). \tag{4.6}$$

Delta function extracts angular part

$$\delta(\varepsilon_k - \varepsilon_{k-q} + E_q) \cong \frac{2m^*}{q}\delta(\cos\theta_{kq} - \Gamma m^*q/k), \tag{4.7}$$

where m^* denotes basic effective mass of band electron.

Integral over the angular part $d\Omega_q$ is removed, and IP remains:

$$\operatorname{Im}\tilde{\varepsilon}_k \cong C_2\rho_0^2\xi^2\int \gamma_2(k, q)n_B(E_{k-q})L(\Gamma m^*q)q^2 dq \propto \tau_k^{-1}, \tag{4.8}$$

where $L(x)$—linear function, τ—relaxation time.

We can extend the next quantities in a limit of small energies of CBF of Bose function

$$n_B(E) \cong 1/\beta E, \quad L \propto \Gamma m^*, \quad \gamma_2(k, q) \cong \gamma_2 = \text{const}, \tag{4.9}$$

and average frequency of scattering of the band electrons

$$\tau^{-1} = \frac{1}{N}\sum_k \operatorname{Im}\varepsilon_k \cong \rho_0^2\xi^2 T I_\tau, \text{ where } I_\tau = \int q^2 dq \frac{\gamma_2 q}{(q-k)^2}: \tag{4.10}$$

for $T > T_{c+}$,

$$\xi^2(T) \propto T - T_{c-}, \quad \Delta\tau^{-1}(T_{c+}) = \tilde{I}_\tau\rho_0^2(T_{c+} - T_{c-})T_{c+}, \tag{4.11}$$

where averaged value $\tilde{I}_\tau$ for (4.10) is introduced. According to the Drude formula for ER (R),

$$\Delta R(T_{c+}) \propto T_{c+}(T_{c+} - T_{c-}) = T_{c+}\Delta T_h, \tag{4.12}$$

i.e. repeatedly observed ER jump after α–γ-transition, ΔR, is proportional, according to Eq. (4.12), to the loop width ΔT_h of temperature

hysteresis of this transition.

5. GENERALIZATION OF THE THEORY FOR Ce-ALLOYS ON THE EXAMPLE OF $Ce_{1-x}Al_x$

Admixtures of nonmagnetic metals modify lattice of alloy and mechanisms of transition. Leaving aside the $4f-3d$-alloys, let us specify only the appearance of new effects for them, unexpected as for pure $3d$-, and for $4f$- (REM) metals. One of them is the change in the critical temperatures (and mechanisms of transition) as a function of concentration x. The changes in magnetic phase diagrams (MPD) [10, 11, 4] are the most technically important ones. Even for nonmagnetic alloys Ce−Yb and Ce−Al $(3s^3 3p^1)$, interesting peculiarities for behaviour of the lattice phase diagrams (LPD) are experimentally revealed [8]. Here, we (qualitatively) correlate data in Ref. [8] with electronic structure of Ce−Al alloys and bonds in them: covalent (of ions), band (metallic), and band−covalent ones.

Except of the wave function for Ce, $\psi_r(Ce)$ (1.1), we introduce wave function of Al ion:

$$\psi_r^+(Al) = \xi_v V_r + \xi_0 \psi_r^+(Al^0) + \sum_\sigma \xi_{b\sigma} f_{r\sigma}^+, \quad V_r = V_0 + \sum_k V_k e^{ikr}, \qquad (5.1)$$

with amplitudes of the states of ion and atom (Al^+ and Al^0) and band fermions $f_{r\sigma}$. The MEOS for Al^+ ion including locality condition [4]

$$V_r = \{V_{r\sigma} c_{r\sigma}\}, \quad [V_k, V_q]_+ = \delta_{kq}/Nx\xi_v^2. \qquad (5.1')$$

Without considering MPD for Ce alloys, we omit the spin index σ.

Considering (CBF and band) spectra for the Hamiltonian terms of different order, we introduce factors $(1 - x)^p$ for $p = 1, 2, ...,$ and add functional V_r:

$$\Delta H^{cov} = -x^2 \sum_{rR} \xi_v^2 \Gamma^{vv} V_r \overline{V}_R - (1 - x)x\xi_d\xi_v \sum_{rRt}(\Gamma^{dv}D_r\overline{V}_R\overline{V}_t + H.c.) -$$
$$-\xi_d\xi_v(1 - x)x(\Gamma^{dve}D_r\overline{V}_R f_R + H.c.) - x\xi_v \sum_{rR}(\gamma_v V_r f_R + H.c.). \qquad (5.2)$$

In the **k**-representation (z_{ij}—coordinate numbers):

$$H = H_0 + \sum_k H_k,$$
$$H_0/N = -\xi_d^2 \Gamma^{dd}(1 - x)^2 - x^2\xi_v^2\Gamma^{vv} - (1 - x)x\xi_d\xi_v\Gamma^{dv}z_{dv}. \qquad (5.3)$$

Term H_0 is added to TDP for

$$\xi_d = \xi, \quad \xi_v \cong 1, \qquad (5.4)$$

i.e.

$$\Phi = \Phi_0 + \Delta\Phi^{c\text{-}b}, \tag{5.5}$$

including band−covalent term

$$\Delta\Phi^{c\text{-}b} = -\gamma_d \xi_d(1-x) - (1-x)x\xi_d\Gamma^{dve}K_{dve}, \tag{5.6}$$

where the introduced correlator (which will be calculated separately)

$$K_{dve} = \left\langle D_0 \bar{V}_k f_k \right\rangle, \tag{5.7}$$

allows finding the change of the critical temperature $T_{c+}(x)$ and width of hysteresis $\Delta T_h(x)$.

Introduce a renormalization (at $x \neq 0$) for band−covalent term γ, which is crucial for ΔT_h,

$$\tilde{\gamma}(x) = \gamma_d + xK_{dve}\gamma_{dve}. \tag{5.8}$$

Varying TDP as in Sec. 2, one can obtain

$$\xi^2 U_d = (I_d/\beta)(1-x) - \tilde{E}_{4f} + \tilde{\gamma}(x)/2\xi. \tag{5.9}$$

We observe a drop of the fixed α−γ-transition temperature,

$$T_{c+}(x) = T_{c+}(0)(1-x), \quad T_{c+}(0) = \tilde{E}_{4f}/I_d k_B, \tag{5.10}$$

and (maximal) width of hysteresis,

$$\Delta T_h(x) = \tilde{\gamma}^{2/3}(x)U_0^{1/3}/k_B \cong \Delta T_h(0)(1 - xK_{dve}|\gamma_{dve}|/\gamma_d). \tag{5.11}$$

Generally, decrease or increase in the hysteresis width depends on the signs of γ_d and γ_{dve}.

However, $\Delta T_h(x)$ is affected more strongly by the character of domains in α−γ-phases, *i.e.* by the transition mechanism. Note also that (Fig. 2) conclusion (5.10) agrees with data in Ref. [8] for Ce−Al. Agreement of (5.11) with data in Ref. [8] is not so unambiguously caused by influence of character of domains.

6. SUMMARY AND CONCLUSIONS

The h.c.p. symmetry of almost all REM can be explained only by the many-electron quantum statistics methods. One can divide the bonding forces of REM (as usually) on band (of 6s-electrons) and covalent ones in a form of MEOS [4]. Since the number of 6s-electrons ($n_b^s = 2$) is un-

changed in REM series, their band energies E_b can consider as equal. Covalent energy of REM (2.3) is

$$H^{\mathrm{cov}} \cong H_0 = -\xi_f^2 \sum_{k\sigma} \Gamma^{ff} F_0 f_{k\sigma}^+ \bar{F}_0 f_{k\sigma} \cong -\Gamma^{ff} n_b^s n_f \cong -E_f n_f, \qquad (6.1)$$

since

$$F_0 \bar{F}_0 \xi_f^2 \cong n_f \text{ for } \xi_f^2 \cong 1 \text{ (except Ce).} \qquad (6.2)$$

Number of $4f$-electrons ($2 < n_f \le 13$) rises as REM number rises that linearly increases contribution of (6.1) into the bonding energy.

Let us compare result (6.1) with experimental data [9] for melting (T_L) and Debye (T_D) temperatures (Fig. 3). We use relation

$$k_B T_L \cong E_b + E_f n_f, \quad E_b/k_B \cong 1.2 \cdot 10^3 \text{ K}, \quad E_f \cong 0.5 \cdot 10^2 \text{ K.} \qquad (6.3)$$

Analogously, one can explain linear rise of T_D [9] on n_f. Exceptions to the rules (6.3) in REM series,—Eu, Yb, and Ce,—are caused by $\xi_f \to 0$ for $n_f = 7$ (Eu), $n_f = 14$ (Yb) and Ce ($4f \to 5d$). Their lattices preserve the f.c.c. symmetry since simultaneously have $\mathbf{J} = \mathbf{0}$. The case of Lu ($4f^{14}5d^1$) confirms given theory by inclusion of $5d-5d$-bonds as (6.1) type and others, and in this case $T_L(\mathrm{Lu}) \cong T_L(\mathrm{Ta})$.

The paradoxical nature of Ce ($4f^2$) is that spin (exchange) component of the bond (6.1), which delocalizes $4f$-electrons of Ce, annihilates both spin S_r and orbital moment L_r. That is why even $\alpha-\gamma$-transition is isomorphic (f.c.c.–f.c.c.). Thermal effect is realized by the excitation of CBF represented by the Fourier transformations of MEOS. The jump of
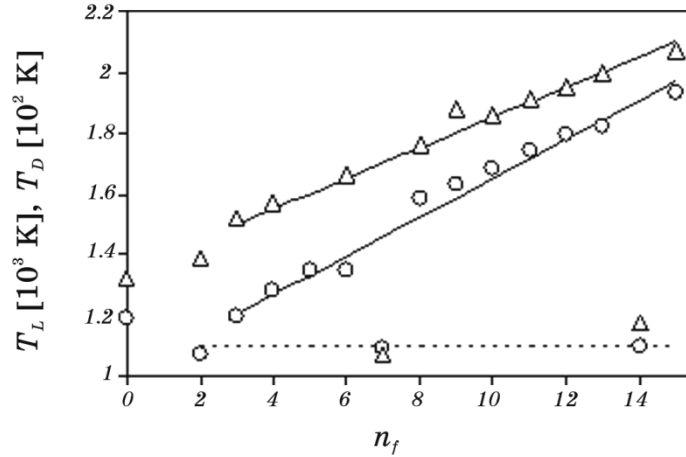
Fig. 3. Melting $T_L(n_f)$ (○) and Debye $T_D(n_f)$ (△) temperatures *vs.* the $4f$-electron number (n_f). Lines—theory (6.1), ○ and △—experimental data [9].

amplitude $\xi_d(T)$ results to the volume jump $\Delta\omega(T)$ (which is connected with covalent $5d$–$5d$-bond energy Γ^{dd}) and leads to the jumps of entropy ΔS and ER (also observed experimentally). However, width of hysteresis ΔT_h of the first-order transition is caused by the band-covalent energy γ_{b-c}. General theory [1, 9] connects first-order transition mechanism with transition domain structure. Therefore, real (experimental) values of the jumps will be estimated in another study.

Earlier revealed jumps $\Delta R \sim 10^{-4}\Omega$, (see Ref. [12]), as well as pressure effect on this isomorphic α–γ-transition in Ce [13], attracted a considerable interest.

The role of cycling for trend of ER $R(T)$ during α–γ-transition process [14], diffraction of electron backscattering [15], electron–positron annihilation [16], high-pressure effect on $R(T)$ [17] are studied.

Observations of new phase boundaries [18] and anomalous behaviour of Grüneisen parameter [19] somehow deal with transition domain structure.

Theoretical studies of Ce were still limited to either phenomenological models (which involved $4f$–$5d$-transition) or single-electron (band) calculations [20]. Among recent works, we note review [21] of theories for ion states in the seven phases of Ce, single-electron calculation [22] at $T = 0$ K, and analysis [23] of change in valence $Ce^{3+,4+}$ of Ce–(O, Au) film. Note also data for $Ce_{75}Al_{25}$ [24] for pressures up to 5 GPa.

We conclude as follows.

1. The MEOS method allows expressing of the hexagonal distortions of REM via the angular moment **J** (of REI) in agreement with experiment ($\Delta(c/a) \propto J_z^2$).

2. Within the scope of the MEOS, indirect covalent $4f$–($6s$)-interaction of REI via the band ($6s$-fermions) parts adds to the metallic bond energy E_b term $E_{4f} \propto n_f$ ($2 < n_f \leq 13$) interpreting behaviour of the melting $T_L(n_f)$ and Debye $T_D(n_f)$ temperatures.

3. Smallness of $n_f = 2$ contributes to the partially covalent delocalization of $4f$-electrons and zeroing of spin (**S**$_r$) and orbital (**L**$_r$) moments of Ce. This 'paradox' removes the hexagonal distortion (**J** = **0**) of REM series, makes stable f.c.c. symmetry and lowers E_{4f}.

4. Instability of partially delocalized $4f$-shell allows the appearance of $5d$-electrons. Additional covalent $5d$–$5d$-bond (Γ^{dd}) manifests itself during increase of T as a CBF result.

5. Screened $\Gamma^{dd}(\mathbf{k})$-bond and its CBF (within the MEOS method) surmount the barrier of $4f$-shell and increase the volume by $\Delta\omega \cong 0.1$ at a jump of α–γ-transition.

6. Its hysteresis (h) with maximal width $\Delta T_h \propto \gamma_{b-c}^{2/3}$ is expressed by the γ_{b-c} parameter of band–covalent bond that gives $\Delta\omega_h \propto \Delta T_h$.

7. Transition entropy $\Delta S \propto \Delta T_h$ is determined by the jump of $5d$-amplitude $\xi_d(T)$ of the wave function of REI $\Delta\xi(T_{c+})$ near the transition

temperature $T \cong T_{c+}$.

8. Transition jump of ER in a form $\Delta R(T_{c+}) \propto \Delta T_h$ is caused by the scattering of band fermions on CBF.

9. Impurities (Al_x, ...) decrease $T_{c+}(x)$ and $\Delta T_h(x)$ and affect other properties of Ce$-$Al via the change in $\xi_d(T,x)$ and CBF spectrum.

REFERENCES

1. S. V. Vonsovsky, *Magnetism* (Moscow: Nauka: 1971) (in Russian).
2. Yu. P. Irkhin and V. Yu. Irkhin, *Elektronnoe Stroenie i Fizicheskie Svoystva Perekhodnykh Metallov (Electron Structure and Physical Properties of Transition Metals)* (Sverdlovsk: Ural State University: 1989) (in Russian).
3. A. I. Mitsek and V. N. Pushkar', *Real'nye Kristally s Magnitnym Poryadkom (Real Crystals with Magnetic Order)* (Kiev: Naukova Dumka: 1978) (in Russian).
4. O. I. Mitsek, *Uspehi Fiziki Metallov*, **13**, No. 4: 345 (2012) (in Russian).
5. G. P. Brekharya, O. A. Kharitonova, and T. V. Gulyayeva, *Uspehi Fiziki Metallov*, **15**, No. 1: 35 (2014) (in Russian).
6. O. I. Mitsek and V. M. Pushkar, *Metallofiz. Noveishie Tekhnol.*, **34**, No. 6: 721 (2012) (in Russian).
7. O. I. Mitsek and V. M. Pushkar, *Metallofiz. Noveishie Tekhnol.*, **36**, No. 1: 103 (2014) (in Russian).
8. Yu. M. Koval' and S. O. Ponomaryova, *Metallofiz. Noveishie Tekhnol.*, **34**, No. 3: 359 (2012) (in Russian).
9. K. N. R. Taylor and M. I. Darby, *Physics of Rare Earth Solids* (London: Chapman and Hall LTD: 1972).
10. K. P. Belov, M. A. Belyanchikova, R. Z. Levitin, and S. A. Nikitin, *Redkozemel'nye Ferro- i Antiferromagnetiki (Rare-Earth Ferro- and Antiferromagnetics)* (Moscow: Nauka: 1965) (in Russian).
11. K. P. Belov, *Redkozemel'nye Magnetiki i Ikh Primenenie (Rare-Earth Magnetics and Their Application)* (Moscow: Nauka: 1980) (in Russian).
12. F. H. Spedding, A. H. Daane, and K. W. Herrmann, *Metals J.*, **9**, No. 4: 895 (1957).
13. N. N. Sirota and A. V. Morozov, *Doklady RAN*, **402**, No. 5: 2005 (613) (in Russian).
14. R. W. Major and T. E. Leinhardt, *J. of Physics and Chemistry of Solids*, **28**, No. 9: 1669 (1967).
15. C. J. Boehlert, J. D. Farr, R. K. Schulze, R. A. Pereyra, and J. A. Archuleta, *Philosophical Magazine*, **83**, No. 14: 1735 (2003).
16. J. M. Leger, *Phys. Lett.*, **57 A**, No. 2: 191 (1976).
17. R. F. Gempel, D. R. Gustafson, and J. D. Willenberg, *Phys. Rev. B*, **5**, No. 6: 2082 (1972).
18. E. King, J. A. Lee, I. R. Harris, and T. F. Smith, *Phys. Rev. B*, **1**, No. 4: 1380 (1970).
19. R. Ramirez and L. M. Falikov, *Phys. Rev. B*, **3**, No. 8: 2425 (1971).
20. J. Ramakrishnan and G. C. Kennedy, *J. Appl. Phys.*, **51**, No. 10: 2586 (1980).
21. A. V. Nikolaev and A. V. Ivashchenko, *Uspekhi Fizicheskikh Nauk*, **182**, No. 7: 701 (2012) (in Russian).

22.   N. Lanata, Y.-X. Jao, C.-Z. Wang, K.-M. Ho, J. Schmalian, K. Haule, and
       G. Kotliar, *Phys. Rev. Lett.*, **111**, No.19: 196801 (2013).
23.   Y. Pan, N. Nilius, H.-J. Freund, J. Paier, Ch. Penschke, and J. Sauer,
       Phys. Rev. Lett., **111**, No. 20: 206101 (2013).
24.   G. Li, Y. Y. Wang, P. K. Liaw, Y. C. Li, and R. P. Liu, *Phys. Rev. Lett.*, **109**,
       No. 12: 125501 (2012).